Analysis of Indium Oxidation State on the Electronic Structure and Optical Properties of TiO$_2$

Matiullah Khan [1,2,3] [iD]**, Zhenghua Lan [2] and Yi Zeng [1,*]**

[1]   State Key Lab of High Performance Ceramics and Superfine Microstructure, Shanghai Institute of Ceramics, Chinese Academy of Sciences, Shanghai 200050, China; matiullahustb@gmail.com
[2]   Shanghai Career Metallurgy Furnace Material Co., Ltd., Shanghai 201908, China; lanzhenghua716@163.com
[3]   Department of Physics, Kohat University of Science and Technology (KUST), Kohat 26000, Pakistan
[*]   Correspondence: zengyi@mail.sic.ac.cn; Tel.: +86-021-5241-2107

check for updates

Abstract: Due to the high formation energy of Indium interstitial defect in the TiO$_2$ lattice, the most probable location for Indium dopant is substitutional sites. Replacing Ti by In atom in the anatase TiO$_2$ shifted the absorption edge of TiO$_2$ towards visible regime. Indium doping tuned the band structure of TiO$_2$ via creating In 5p states. The In 5p states are successfully coupled with the O 2p states reducing the band gap. Increasing In doping level in TiO$_2$ improved the visible light absorption. Compensating the charge imbalance by oxygen vacancy provided compensated Indium doped TiO$_2$ model. The creation of oxygen vacancy widened the band gap, blue shifted the absorption edge of TiO$_2$ and declined the UV light absorption. The 2.08% In in TiO$_2$ is the optimal Indium doping concentration, providing suitable band structure for the photoelectrochemical applications and stable geometrical configuration among the simulated models. Our results provide a reasonable explanation for the improved photoactivity of Indium doped TiO$_2$.

Keywords: Indium doped TiO$_2$; oxidation state; doping concentration; optical response

1. Introduction

Environmental pollution and energy crises are the major problems attracting considerable attention from researchers. A semiconductor like Titanium dioxide (TiO$_2$) could be used for environmental cleanup and renewable energy sources [1,2]. However, the wide band gap limits the efficiency of TiO$_2$ in photoelectrochemical applications. With the help of Plasmonic nanoparticles, the limited absorption of TiO$_2$ can be resolved [3,4]. However, for most practical applications, the usage of expensive metal nano-particles is not economically feasible. Doping foreign atoms in the network of TiO$_2$ could be a suitable way to tune the band gap utilizing majors part of the solar spectrum [5,6]. The proper oxidation state of the dopant atoms can favorably stabilize the system and tailor the band structure. Inducing dopant atoms in any semiconductor materials disturbs the structure of the bulk material and the modification depends upon the difference in the ionic radii of bulk and dopant ions. Wide functionalities of the TiO$_2$ could be induced by selecting a dopant with the proper oxidation state. Thus, the band structure of TiO$_2$ could be tuned to utilize a major part of the solar energy with minimum structure distortion [7–10].

Introducing foreign atoms into the bulk of TiO$_2$ either creates states in the forbidden region or mixes with the valence or conduction band modifying the electronic band structure [11,12]. Doping non-metal extended the absorption edge of TiO$_2$ towards a visible regime by creating impurity states (in the forbidden region) or narrowing the band gap [13–15]. The states due to nitrogen (N) appeared above the valence band maximum which might annihilate the photo-generated carriers [16]. The efficiency of transition metals doped TiO$_2$ is also limited due to the existence of localized d states

and the recombination centers [17]. Existence of the isolated states in the band gap effect the optical absorption spectra and photo-activity of TiO_2. Unoccupied isolated states often act as an electron trap, promoting the electron-hole pair recombination [18,19]. Removing the unoccupied states from the band gap or mixing it with the valence or conduction band would increase the lifetime of the photo-excited carriers, thereby improving the photo-activity.

Mixing the oxide of Indium (In) with TiO_2 and improving the photo-activity are widely reported in literature. Nanocrystalline TiO_2-In_2O_3 powders with different Ti/In ratios are prepared by sol-gel method and the photodegradation response is evaluated. Mixing In_2O_3 with TiO_2 improved the photoelectrochemical properties of TiO_2 [20]. The photoactive In_2O_3-TiO_2 mixed oxides are extensively studied by Gonzalez et al. [21] and the photocatalytic activity are explored. The Indium oxide (In_2O_3) in combination with the silver improved the photoactivity of TiO_2 [22]. Wang et al. [23] prepared Indium doped TiO_2 by the sol-gel method and evaluated the photo-activity under visible light illuminations. Doping Indium in the TiO_2 lattice improved the activity for the degradation of 4-chlorophenol under visible light irradiations. The topic of mixing the In_2O_3 with TiO_2 or doping Indium in the structure of TiO_2 is experimentally investigated. However, the alterations in the band structure and lattice of TiO_2 due to Indium doping are rarely reported. To elucidate the effect of Indium doping on the geometrical structure, band structure and photo-response, it is suggested to perform some ab-initio calculations.

This work report DFT based calculations for Indium (In) doped TiO_2 with different In doping level. Charge neutralization is made by generating oxygen vacancy and the electronic band structure and optical properties are evaluated.

2. Method of Calculations

With Materials Studio 8.0, the calculations are performed based on the plane wave method of DFT. The generalized gradient approximation (GGA) parameterized by PBE is utilized as an exchange correlation potential [24]. Keeping the maximum energy equal to 400 eV and k-mesh of $2 \times 2 \times 2$, the electrons wave functions are expanded (in plane waves). The simulation environment is the ideal environment which is relaxed using some constraints for optimizing the simulated models. Using the BFGS minimization scheme [25], the maximum displacement was set to 5.0×10^{-4} Å, while the convergence limit for self-consistent tolerance was 2.0×10^{-6} eV/atom.

Anatase TiO_2 supercell is made from the replication of $2 \times 2 \times 1$ TiO_2 unitcell. Low concentration of Indium in anatase TiO_2 are possible by increasing the size of the supercell. Indium (In) doped models are constructed by replacing the lattice Ti atoms by In atoms. Doping single In atom at Ti sites have the In doping level of 2.08% represented by $Ti_{16-1}In_1O_{32}$. The doping concentration of In is increased to 4.16% and this system is named as $Ti_{16-2}In_2O_{32}$. The effect of oxygen vacancy on the band structure is evaluated by creating one oxygen vacancy along with two In atoms at Ti sites and it is represented by $Ti_{16-2}In_2O_{31}$. Figure 1 displays the atomic configuration of anatase TiO_2 having substitutional In (at Ti site) and oxygen vacancy. As a standard model, a defect free bare TiO_2 is also simulated.
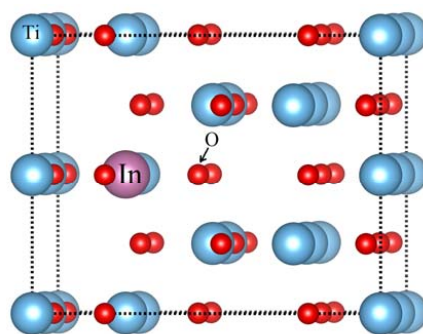

Figure 1. Insertion of Indium atom at Ti site in anatase TiO_2 network.

3. Results and Discussion

The calculated lattice parameters for pure TiO_2 (anatase) are; a = 3.81 Å and c = 9.71 Å, compared to the reported theoretical (a = 3.81 Å and c = 9.48 Å) [26] and experimental data (a = 3.78 Å and c = 9.49 Å) [27]. The bond lengths of the optimized systems are averaged and shown in Table 1. The O-Ti and O-O bonds are 1.9651 and 2.7034 Å, respectively. The $Dmol^3$ based calculated Ti-O bond length for pure TiO_2 is reported to be 1.930 Å [28]. Treacy et al. [29] studied the structural features of anatase TiO_2 (101) with surface x-ray diffraction (SXRD) and then compared the results with the calculations based on density functional theory (DFT). It is found that the Ti-O bond length fluctuates between 1.89 ± 0.01 Å and 2.08 ± 0.01 Å [29]. Inducing defects modified the averaged bond lengths of the optimized TiO_2. The bonds of $Ti_{16-1}In_1O_{32}$ are stretched compared to the bare TiO_2 which might be due to the replacement of lattice Ti by In atom. Increasing the Indium doping concentration further elongates the O-Ti bond length of the $Ti_{16-2}In_2O_{32}$, however, the O-O bond length is reduced relative to the TiO_2 and $Ti_{16-1}In_1O_{32}$. Furthermore, the D_{O-In} of the $Ti_{16-2}In_2O_{32}$ is also stretched with respect to $Ti_{16-1}In_1O_{32}$. Oxygen vacancy has an interesting influence on the bond lengths of the doped models. With the same doping concentration, the D_{O-Ti} of the $Ti_{16-2}In_2O_{31}$ is reduced while the D_{O-O} is elongated compared to $Ti_{16-2}In_2O_{32}$. In addition, the D_{O-In} bond length showed no considerable variation. Modifications in the bond lengths of defect induced models are attributed to the different ionic radii of Ti^{4+} (68 pm) and In^{3+} (81 pm) [30,31]. Comparing the relative changes induced in the bond lengths due to different doping configuration, the $Ti_{16-1}In_1O_{32}$ modelled system provided minimum structure distortion in reference to bare TiO_2. This system might improve the stability of the doped TiO_2 system and further improve the efficiency of In-doped in photoelectrochemical applications.

**Table 1.** Bond lengths (averaged) of the simulated models.

Bond Length	TiO_2	$Ti_{16-1}In_1O_{32}$	$Ti_{16-2}In_2O_{32}$	$Ti_{16-2}In_2O_{31}$
D_{O-Ti} (Å)	1.9651	1.9721	1.9846	1.9755
D_{O-O} (Å)	2.7034	2.7152	2.6886	2.7547
D_{O-In} (Å)	—	2.1294	2.1707	2.1723

The electronic band structure of the simulated models is depicted in Figure 2. The DFT based theoretically calculated electronic band gap is associated with the photoemission data. Similarly, the optical gap in the form of direct band gap could be linked with the spectrum of excitonic effects. The absorption spectrum of the TiO_2 has a relationship with the optical band gap. Therefore, the spectrum of the TiO_2 can be tuned by doping various elements, which create states in band gap or mix with valence or conduction band [5,32,33]. The calculated band gap of pure TiO_2 (2.13 eV) is underestimated relative to the 3.20 eV. The underestimation is a drawback of GGA based calculations [34]. In case of known exact exchange-correlation potential, the DFT can only have access to the ground state properties. To deal with this problem, the electronic excitations modeled by Kohn-Sham equations should be substituted by the Dyson equation. Thus, the unknown exchange-correlation potential is modeled by an operator depending on the self-energy. The utilization of the Hubbard model along with DFT is one of the ways to deal with the underestimated band gap [10,35,36]. We consider the current study as a relative study that describes the relative changes induced due to different doping/defect configurations. So, the underestimation would not affect our results. Replacing the lattice Ti atom by In atom ($Ti_{16-1}In_1O_{32}$), the band gap is reduced to 2.113 eV. The reduction in the band gap would be helpful in shifting the absorption regime towards visible light. Moreover, the Fermi level is moved slightly upwards in the forbidden region. The location of the Fermi level and the band edge positions of different models are summarized in Table 2. At gamma point, the band gap of $Ti_{16-2}In_2O_{32}$ is 2.65 eV. Though the band gap seems to be extended, some humps are present at the conduction band maximum and it may help in migrating the electrons from valence to conduction band. Creating oxygen vacancy widens the band gap and the band gap for $Ti_{16-2}In_2O_{31}$

is 2.483 eV. The widening of the band gap due to oxygen vacancy in TiO_2 is consistent with literature and this increase might be explained by the localized states [37,38].

Table 2. Band edge and Fermi level positions in different systems. The valence band maximum and conduction band minimum are represented by VBM and CBM, respectively.

	TiO_2	$Ti_{16-1}In_1O_{32}$	$Ti_{16-2}In_2O_{32}$	$Ti_{16-2}In_2O_{31}$
Fermi level (eV)	Above VBM	0.25 eV above VBM	0.1 eV below VBM	0.1 eV above VBM
VBM (eV)	0	−0.75	0.1	−0.92
CBM (eV)	2.13	1.85	2.75	2.40
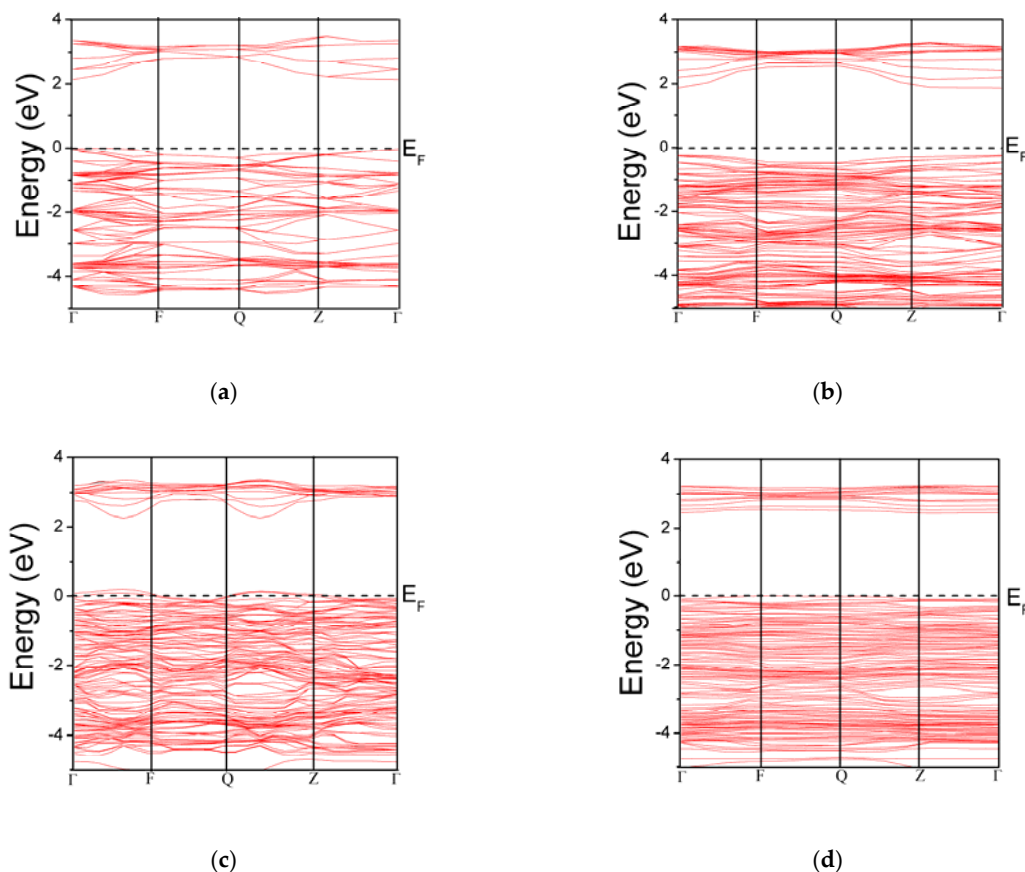
Figure 2. Band structure of TiO_2 and defect induced models: (**a**) TiO_2; (**b**) $Ti_{16-1}In_1O_{32}$; (**c**) $Ti_{16-2}In_2O_{32}$; and (**d**) $Ti_{16-2}In_2O_{31}$.

The band structure modifications are further investigated and densities of states are calculated. Figure 3 displays the density of states of the simulated models. Doping In atoms modified the band structure of TiO_2 and the In 5p states are coupled with the host O 2p and Ti 3d states. Increasing the In doping level from 2.08% to 4.16% has no considerable effect on the band gap. Figure 3b demonstrates the partial density of states (PDOS) of the models. It is clarified that the valence band of bare TiO_2 comprises of O 2p states while the Ti 3d contribute (predominantly) to the conduction band. Adding In atoms at Ti sites induced In 5p states which are coupled with the O 2p states, modifying the valence band of TiO_2. In the $Ti_{16-2}In_2O_{32}$ model, the Indium doping concentration is increased to 4.16% and the density of In 5p states near the valence band is enhanced. Moreover, some In 5p also contribute to modifying the conduction band. The intensity of In 5p states in the $Ti_{16-2}In_2O_{31}$ model remains the same. However, the In 5p states are smoothened compare to the non-compensated systems. The In 5p

states in the band structure would be supportive in migrating the visible light photons from valence to conduction band.
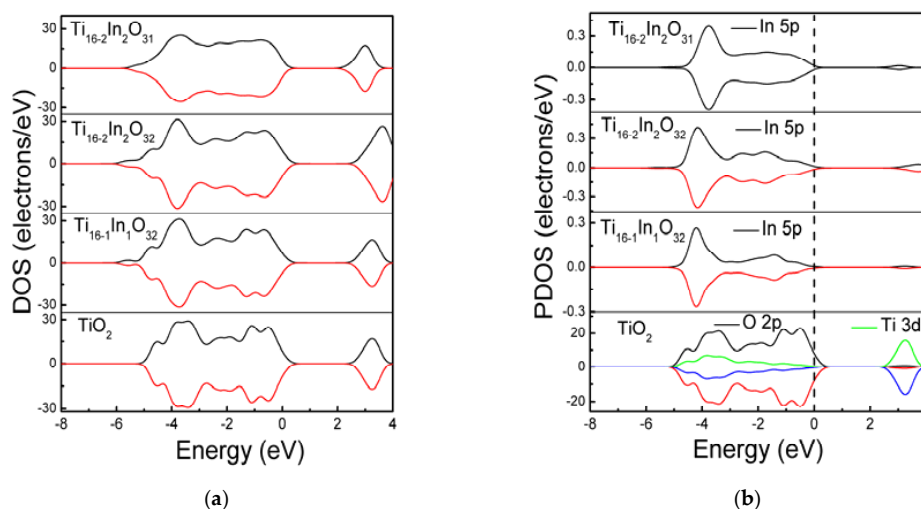
Figure 3. The (**a**) total density of states and; (**b**) partial density of states.

Figure 4 depicts the optical absorption spectra of the simulated systems. Tuning the band structure modifies the optical absorption properties of the semiconductor materials. For evaluating the optical properties, the underestimated band gap is updated to the experimental value of the band gap (3.20 eV) with scissor approximation [12]. The spectrum of bare TiO_2 displays absorption in the UV region only because the wide band gap deprives it from utilizing the major part of the solar energy. The UV light absorption corresponds to the excitations of electron between O 2p and Ti 3d states. The In doping in the anatase TiO_2 network shifted the absorption range towards the visible regime. It is clarified from Figure 4 that with the UV absorption, the $Ti_{16-1}In_1O_{32}$ model also exhibits visible light absorption. The In 5p states are responsible for shifting the absorption threshold towards visible light region. In this case, the electron undergoes step wise transition from O 2p to Ti 3d states via In 5p states. Thus, it indirectly modifies the absorption spectra. Increasing the Indium doping level improved the absorption in the visible regime. The shifting of the absorption edge of TiO_2 towards visible regime due to In doping is consistent with the reported data [23]. Inducing oxygen vacancy in the Indium doped TiO_2 model made the absorption peak disappear in the visible light region. In addition, the $Ti_{16-2}In_2O_{31}$ model only absorbs UV light, confirming the findings of band structure analysis. Furthermore, the UV light absorption is also reduced compared to bare TiO_2. The $Ti_{16-2}In_2O_{31}$ blue shifted the absorption regime of the TiO_2. Stable structure, favorable band structure and improved optical response of In-doped TiO_2 would improve its efficiency in photoelectrochemical applications.
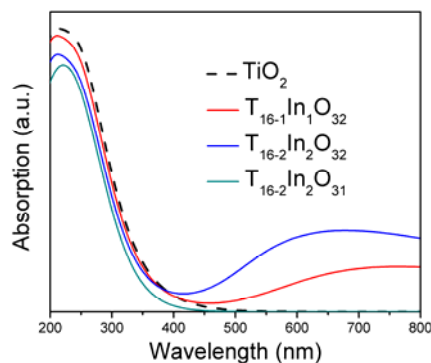
Figure 4. Optical response of the TiO_2 and defect induced TiO_2 models.

4. Conclusions

Substitutional In doping at Ti sites reduced the band gap of anatase TiO_2 and shifted the absorption edge toward the visible regime. Along with the absorption in the visible light region, the absorption in UV regime is also improved in reference to pure TiO_2. The band structure of TiO_2 is modified due to the creation of In 5p states in the band structure. The defect states associated with In are successfully mixed with the O 2p states without creating isolated states in the band gap. Increasing In doping level induced no substantial change in the absorption spectra. The creation of oxygen vacancy in the Indium doped TiO_2 blue shifted the absorption edge and declined the UV light absorption. The experimentally observed improved photoactivity of In-TiO_2 could be reasonably explained by the 2.08% In doped TiO_2 model, which exhibits stable configuration, and reduced band gap. The proper oxidation state of In dopant stabilized the TiO_2 system while inducing visible light absorption spectrum. Stabilizing the visible light active In doped TiO_2 would improve its efficiency in photoelectrochemical applications.

References

1. Papadimitriou, V.C.; Stefanopoulos, V.G.; Romanias, M.N.; Papagiannakopoulos, P.; Sambani, K.; Tudose, V.; Kiriakidis, G. Determination of photo-catalytic activity of un-doped and Mn-doped TiO_2 anatase powders on acetaldehyde under UV and visible light. *Thin Solid Films* **2011**, *520*, 1195–1201. [CrossRef]

2. Murphy, A. Does carbon doping of TiO_2 allow water splitting in visible light? Comments on "Nanotube enhanced photoresponse of carbon modified (CM)-n-TiO_2 for efficient water splitting". *Sol. Energy Mater. Sol. Cells* **2008**, *92*, 363–367. [CrossRef]

3. Atsushiro Tanaka, K.H.; Kominami, H. A very simple method for the preparation of Au/TiO_2 plasmonic photocatalysts working under irradiations of visible light in the range of 600–700 nm. *Chem. Commun.* **2017**, *53*, 4759–4762. [CrossRef] [PubMed]

4. Timur, S.H.; Atabaev, M.A.H.; Lee, D.; Kim, H.K.; Hwang, Y.H. Pt-coated TiO_2 nanorods for photoelectrochemical water splitting applications. *Results Phys.* **2016**, *6*, 373–376.

5. Na Phattalung, S.; Limpijumnong, S.; Yu, J. Passivated co-doping approach to bandgap narrowing of titanium dioxide with enhanced photocatalytic activity. *Appl. Catal. B Environ.* **2017**, *200*, 1–9. [CrossRef]

6. Matiullah, K.; Zeng, Y.; Fawad, U.; Wazir, M.; Abdul, N.; Muhammad Iqbal, Z.; Asad, U. Enhancing the photoactivity of TiO_2 by codoping with silver and molybdenum: The effect of dopant concentration on the photoelectrochemical properties. *Mater. Res. Express* **2017**, *4*, 045023. [CrossRef]

7. Zhao, Y.F.; Li, C.; Lu, S.; Gong, Y.Y.; Niu, L.Y.; Liu, X.J. Modulating TiO_2 photocatalyst by Al doping: Density functional theory approach. *Chem. Phys. Lett.* **2016**, *654*, 13–17. [CrossRef]

8. Lazzeri, M.; Vittadini, A.; Selloni, A. Structure and energetics of stoichiometric TiO_2 anatase surfaces. *Phys. Rev. B* **2001**, *63*. [CrossRef]

9. Long, M.; Cai, W.; Wang, Z.; Liu, G. Correlation of electronic structures and crystal structures with photocatalytic properties of undoped, N-doped and I-doped TiO_2. *Chem. Phys. Lett.* **2006**, *420*, 71–76. [CrossRef]

10. Khan, M.; Xu, J.; Chen, N.; Cao, W. Electronic and optical properties of pure and Mo doped anatase TiO_2 using GGA and GGA+U calculations. *Phys. B Condens. Matter* **2012**, *407*, 3610–3616. [CrossRef]

11. Khan, M.; Cao, W. Preparation of Y-doped TiO_2 by hydrothermal method and investigation of its visible light photocatalytic activity by the degradation of methylene blue. *J. Mol. Catal. A Chem.* **2013**, *376*, 71–77. [CrossRef]

12. Cui, Y.; Du, H.; Wen, L. Origin of visible-light-induced photocatalytic properties of S-doped anatase TiO_2 by first-principles investigation. *Solid State Commun.* **2009**, *149*, 634–637. [CrossRef]

13. Venditti, F.; Cuomo, F.; Ceglie, A.; Avino, P.; Russo, M.V.; Lopez, F. Visible Light Caffeic Acid Degradation by Carbon-Doped Titanium Dioxide. *Langmuir* **2015**, *31*, 3627–3634. [CrossRef] [PubMed]

14. Ren, W.; Ai, Z.; Jia, F.; Zhang, L.; Fan, X.; Zou, Z. Low temperature preparation and visible light photocatalytic activity of mesoporous carbon-doped crystalline TiO_2. *Appl. Catal. B Environ.* **2007**, *69*, 138–144. [CrossRef]

15. Daghrir, R.; Drogui, P.; Robert, D. Modified TiO_2 for Environmental Photocatalytic Applications: A Review. *Ind. Eng. Chem. Res.* **2013**, *52*, 3581–3599. [CrossRef]

16. Khan, M.; Gul, S.R.; Li, J.; Cao, W. Variations in the structural, electronic and optical properties of N-doped TiO_2 with increasing N doping concentration. *Mod. Phys. Lett. B* **2015**, *29*, 1550022. [CrossRef]

17. Štengl, V.; Bakardjieva, S. Molybdenum-Doped Anatase and Its Extraordinary Photocatalytic Activity in the Degradation of Orange II in the UV and vis Regions. *J. Phys. Chem. C* **2010**, *114*, 19308–19317. [CrossRef]

18. Etacheri, V.; Seery, M.K.; Hinder, S.J.; Pillai, S.C. Highly Visible Light Active $TiO_{2-x}N_x$ Heterojunction Photocatalysts†. *Chem. Mater.* **2010**, *22*, 3843–3853. [CrossRef]

19. Di Valentin, C.; Finazzi, E.; Pacchioni, G.; Selloni, A.; Livraghi, S.; Paganini, M.C.; Giamello, E. N-doped TiO_2: Theory and experiment. *Chem. Phys.* **2007**, *339*, 44–56. [CrossRef]

20. Shchukin, D.; Poznyak, S.; Kulak, A.; Pichat, P. TiO_2-In_2O_3 photocatalysts: Preparation, characterisations and activity for 2-chlorophenol degradation in water. *J. Photochem. Photobiol. A Chem.* **2004**, *162*, 423–430. [CrossRef]

21. Rodríguez-González, V.; Moreno-Rodríguez, A.; May, M.; Tzompantzi, F.; Gómez, R. Slurry photodegradation of 2,4-dichlorophenoxyacetic acid: A comparative study of impregnated and sol–gel In_2O_3–TiO_2 mixed oxide catalysts. *J. Photochem. Photobiol. A Chem.* **2008**, *193*, 266–270. [CrossRef]

22. Yang, X.; Wang, Y.; Xu, L.; Yu, X.; Guo, Y. Silver and Indium Oxide Codoped TiO_2 Nanocomposites with Enhanced Photocatalytic Activity. *J. Phys. Chem. C* **2008**, *112*, 11481–11489. [CrossRef]

23. Wang, E.; Yang, W.; Cao, Y. Unique Surface Chemical Species on Indium Doped TiO_2 and Their Effect on the Visible Light Photocatalytic Activity. *J. Phys. Chem. C* **2009**, *113*, 20912–20917. [CrossRef]

24. Jaffe, J.E.; Snyder, J.A.; Lin, Z.; Hess, A.C. LDA and GGA calculations for high-pressure phase transitions in ZnO and MgO. *Phys. Rev. B* **2000**, *62*, 1660–1665. [CrossRef]

25. Pfrommer, B.G.; Côté, M.; Louie, S.G.; Cohen, M.L. Relaxation of Crystals with the Quasi-Newton Method. *J. Comput. Phys.* **1997**, *131*, 233–240. [CrossRef]

26. Jia, L.; Wu, C.; Han, S.; Yao, N.; Li, Y.; Li, Z.; Chi, B.; Pu, J.; Jian, L. Theoretical study on the electronic and optical properties of (N, Fe)-codoped anatase TiO_2 photocatalyst. *J. Alloys Compd.* **2011**, *509*, 6067–6071. [CrossRef]

27. Hou, Y.D.; Wang, X.C.; Wu, L.; Chen, X.F.; Ding, Z.X.; Wang, X.X.; Fu, X.Z. N-doped SiO_2/TiO_2 mesoporous nanoparticles with enhanced photocatalytic activity under visible-light irradiation. *Chemosphere* **2008**, *72*, 414–421. [CrossRef] [PubMed]

28. Xie, K.; Jia, Q.; Wang, Y.; Zhang, W.; Xu, J. The Electronic Structure and Optical Properties of Anatase TiO_2 with Rare Earth Metal Dopants from First-Principles Calculations. *Materials* **2018**, *11*, 179. [CrossRef] [PubMed]

29. Treacy, J.P.W.; Hussain, H.; Torrelles, X.; Grinter, D.C.; Cabailh, G.; Bikondoa, O.; Nicklin, C.; Selcuk, S.; Selloni, A.; Lindsay, R.; et al. Geometric structure of anatase TiO_2 (101). *Phys. Rev. B* **2017**, *95*, 075416. [CrossRef]

30. Khan, M.; Cao, W.; Ullah, M. Ab initiocalculations for the electronic and optical properties of Y-doped anatase TiO_2. *Phys. Status Solidi (B)* **2013**, *250*, 364–369. [CrossRef]

31. Hiroshi, O.; Takeo, S. Selective and Active Transport of In^{3+} through N-Nitroso-N-p-octadecylphenylhydroxylamine Ammonium Salt Impregnated Membrane. *Bull. Chem. Soc. Japan* **1990**, *63*, 920–925.

32. Khan, M.; Yi, Z.; Gul, S.R.; Wang, Y.; Fawad, U. Visible-light-active silver-, vanadium-codoped TiO_2 with improved photocatalytic activity. *J. Mater. Sci.* **2017**, *52*, 5634–5640. [CrossRef]

33. Wang, Y.; Wu, Y.; Yang, H.; Xue, X.; Liu, Z. Doping TiO_2 with boron or/and cerium elements: Effects on photocatalytic antimicrobial activity. *Vacuum* **2016**, *131*, 58–64. [CrossRef]

34. Yu, Q.; Jin, L.; Zhou, C. Ab initio study of electronic structures and absorption properties of pure and Fe^{3+} doped anatase TiO_2. *Sol. Energy Mater. Sol. Cells* **2011**, *95*, 2322–2326. [CrossRef]

35. Long, R.; English, N.J. Electronic properties of F/Zr co-doped anatase TiO^2 photocatalysts from GGA+U calculations. *Chem. Phys. Lett.* **2010**, *498*, 338–344. [CrossRef]

36. Rubio-Ponce, A.; Conde-Gallardo, A.; Olguín, D. First-principles study of anatase and rutile TiO^2 doped with Eu ions: A comparison of GGA and LDA+U calculations. *Phys. Rev. B* **2008**, *78*, doi–10. [CrossRef]

37. Chen, Q.; Tang, C.; Zheng, G. First-principles study of anatase (101) surfaces doped with N. *Phys. B Condens. Matter* **2009**, *404*, 1074–1078. [CrossRef]

38. Fujishima, A.; Zhang, X.; Tryk, D. TiO^2 photocatalysis and related surface phenomena. *Surf. Sci. Rep.* **2008**, *63*, 515–582. [CrossRef]